




Isopimpinellin inhibits UVA-induced overproduction of MMPs via suppression of MAPK/AP-1 signaling in human dermal fibroblasts

Jung Hwan Oh^{1,2} · Fatih Karadeniz¹ · Youngwan Seo³ · Chang-Suk Kong^{1,4} 

Received: 16 January 2024 / Revised: 14 May 2024 / Accepted: 17 May 2024
© The Korean Society of Food Science and Technology 2024

Abstract

Corydalis heterocarpa is an edible halophyte and an ingredient in traditional Korean medicine. In the present study, isopimpinellin (IPN), a bioactive coumarin, was isolated from the medicinal halophyte *C. heterocarpa*, and the effects of IPN against UVA-induced photoaging were investigated in human dermal fibroblasts. Photoaging is a skin disorder that manifests itself as premature skin aging due to chronic exposure to UV radiation. The symptoms of photoaging mainly arise from degraded skin connective tissue produced by overly expressed matrix metalloproteinases (MMPs). IPN treatment decreased the UVA-induced formation of reactive oxygen species and decreased MMP-1, MMP-3, and MMP-9 collagenases at the protein level. The UVA-mediated suppression of tissue inhibitors of MMP-1 and -2 was attenuated with IPN. The presence of 10 μ M IPN inhibited the MAPK-mediated phosphorylation of c-Fos and c-Jun. In conclusion, the overall result of the current study indicated that IPN inhibited the UVA-induced overexpression of MMPs via blocking the MAPK/AP-1 pathway.

Keywords *Corydalis heterocarpa* · Human dermal fibroblast · Isopimpinellin · MMP · Photoaging

Introduction

The human skin acts as a barrier against environmental factors. Its most critical role is the reflection and absorption of ultraviolet (UV) rays, which are relatively harmful and

mutagenic (Narayanan et al., 2010). UV rays have a number of harmful effects on the structure, formation, and integrity of the skin. Continuous exposure to UV rays leads to premature skin aging, also known as photoaging (Salminen et al., 2022). Of the three different wavelength groups of UV rays, UVA (longwave, 315–400 nm), UVB (middle-wave, 280–315 nm) and UVC (shortwave, 100–280 nm), the ozone layer absorbs almost all the UVC and some of the UVB. However, a big part of UVA reaches the earth's surface passing through the atmosphere unobstructed. The unabsorbed UVB can penetrate the epidermis and shallowly, the dermis, the two layers of skin, while UVA can pass through to the basal layer between the skin and the underlying tissue (Meinhardt et al., 2008). Thus, UVA is the major contributor to UV-mediated skin damage, including photoaging (Battie et al., 2014; Wang et al., 2021).

Photoaging of the skin affects the connective tissue of the dermis layer. This layer contains extracellular matrix (ECM) components, such as collagen, that provide the skin with elasticity, strength, and shape. It has been demonstrated that exposure to UVA positively alters the levels of matrix metalloproteinases (MMPs), a family of ECM-degrading enzymes (Herrmann et al., 1993). Excessive levels of MMPs lead to an imbalance in the formation of the ECM by degrading critical components, particularly collagen (Poon et al., 2015).

✉ Chang-Suk Kong
cskong@silla.ac.kr

Jung Hwan Oh
jhoh@silla.ac.kr

Fatih Karadeniz
karadenizf@silla.ac.kr

Youngwan Seo
ywseo@kmou.ac.kr

¹ Marine Biotechnology Center for Pharmaceuticals and Foods, College of Medical and Life Sciences, Silla University, Busan 46958, Republic of Korea

² Nutritional Education, Graduate School of Education, Silla University, Busan 46958, Republic of Korea

³ Division of Convergence on Marine Science, College of Ocean Science and Technology, Korea Maritime and Ocean University, Busan 49112, Republic of Korea

⁴ Department of Food and Nutrition, College of Medical and Life Sciences, Silla University, Busan 46958, Republic of Korea

Decreased collagen synthesis combined with the increased degradation of collagen leads to the collapse of connective tissue, manifested by decreased skin elasticity, wrinkles and the appearance of age spots (Oba et al., 2006; Watson and Griffiths, 2005). MMP-1, and to a certain extent, MMP-3 and MMP-9, are the main enzymes of the MMP family that act on skin collagen and are therefore responsible for the progression of photoaging (Pittayapruet et al., 2016; Quan et al., 2009).

One of the triggers of the photoaging process is the excessive production of reactive oxygen species (ROS) as a result of UV irradiation (Herrling et al., 2006). ROS has been shown to be involved in the signaling mechanisms of photoaging either by directly damaging collagen or by stimulating the expression and activity of MMPs (Ansary et al., 2021). It has been reported that the ROS-induced overproduction of MMPs occurs through the activation of the mitogen-activated protein kinase (MAPK) signaling cascade (Nelson and Melendez, 2004). The MAPK signaling cascade is an intricate phosphorylation pathway involved in several biological reactions. As key components of the MAPK signaling cascade, extracellular signal-regulated kinase (ERK), p38 and c-Jun N-terminal protein kinase (JNK) are widely studied proteins reported to play an active role in the intracellular response to UV exposure (Nelson and Mendez, 2004; Prasanth et al., 2020). The UV radiation-mediated increase in ROS triggers the activation of these MAPK components, which subsequently activate the transcription factor, activator protein 1 (AP-1) (Kong et al., 2022). AP-1 is a transcription factor that triggers the production of MMPs. AP-1 is a heterodimer composed of phosphorylated (p)-c-Fos and c-Jun proteins that are previously activated via p38 and JNK (Kajanne et al., 2007). Therefore, the inhibition of the MAPK/AP-1 signaling cascade is expected to reduce UVA-mediated MMP production, which in turn alleviates the symptoms of photoaging.

Corydalis heterocarpa (*C. heterocarpa*) is a halophyte found throughout Korea and Japan on muddy seashores and coastal dunes. It has been used as an ingredient in traditional folk medicine for several ailments including pain relief. Several bioactivities have been reported for the crude extracts and fractions of *C. heterocarpa*. These include MMP inhibitory (Yu et al., 2021), anti-photoaging (Ahn et al., 2012; Oh et al., 2020a) and anti-inflammatory (Kim et al., 2015) bioactivities. Isopimpinellin (IPN) has been isolated from the active extracts of *C. heterocarpa* as a part of ongoing effort to develop natural-origin anti-photoaging cosmetic agents. IPN is a coumarin derivative, a furanocoumarin, whose anticarcinogenic properties have been demonstrated against certain skin tumors (Kleiner et al., 2002, 2003). In addition, IPN has been shown to exert anti-angiogenic (Bhagavatheswaran et al., 2022), and acetylcholinesterase and self-induced amyloid- β aggregation inhibitory effects (Takomthong et al., 2020). Structure–activity

association studies have indicated that the placement of the furan ring (Takomthong et al., 2020) and the polarizability (Singhuber et al., 2011) of the compound are the main factors for its bioactivity. However, to the best of our knowledge, there is no study available to date in the literature on the effects of IPN against photoaging. In the present study, the potential effects of IPN on UVA-mediated changes in MMP production in human dermal fibroblasts (HDFs) were investigated in vitro to obtain crucial data on its potential use as an anti-photoaging cosmeceutical.

Materials and methods

Isolation and characterization of IPN

Whole *C. heterocarpa* plants were extracted and IPN was isolated among other coumarin derivatives, as previously described (Kim et al., 2015). In the present study, IPN was dissolved in distilled water for use in cell-based experiments. The characterization of the IPN was carried out by comparison of the data below with that in the published literature (Fig. 1A) (Kim et al., 2015).

Maintenance of HDFs

HDFs were procured from PromoCell GmbH (cat. no. C-12302). The cells were cultured in flat-bottom transparent six-well plates with 1×10^6 cells/well seeding density supplemented with fibroblast growth medium (cat. no. C-23020, PromoCell GmbH) unless otherwise indicated. The cultured cells were kept in incubators at 37°C and 5% CO₂ between experiments. Any possible toxic effect of IPN on the HDFs was investigated using a colorimetric MTT assay, as previously described (Kim et al., 2015). Non-toxic concentrations were used for further assays.

Irradiation of HDFs with UVA

Exposure to UVA was carried out using a Bio-Sun UV Irradiation System (Vilber Lourmat). HDFs cultured as described previously were irradiated until the UVA exposure reached the 10 J/cm² dose. Prior to irradiation, the culture medium was changed to phosphate-buffered saline (PBS) and the microplate lid was removed. Following irradiation, the cells were supplemented with DMEM without any serum until analysis.

2',7'-Dichlorofluorescein diacetate (DCFH-DA) assay for the measurement of intracellular radical scavenging activity

The effects of IPN on cellular ROS production were investigated using the ROS-sensitive DCFH-DA assay.

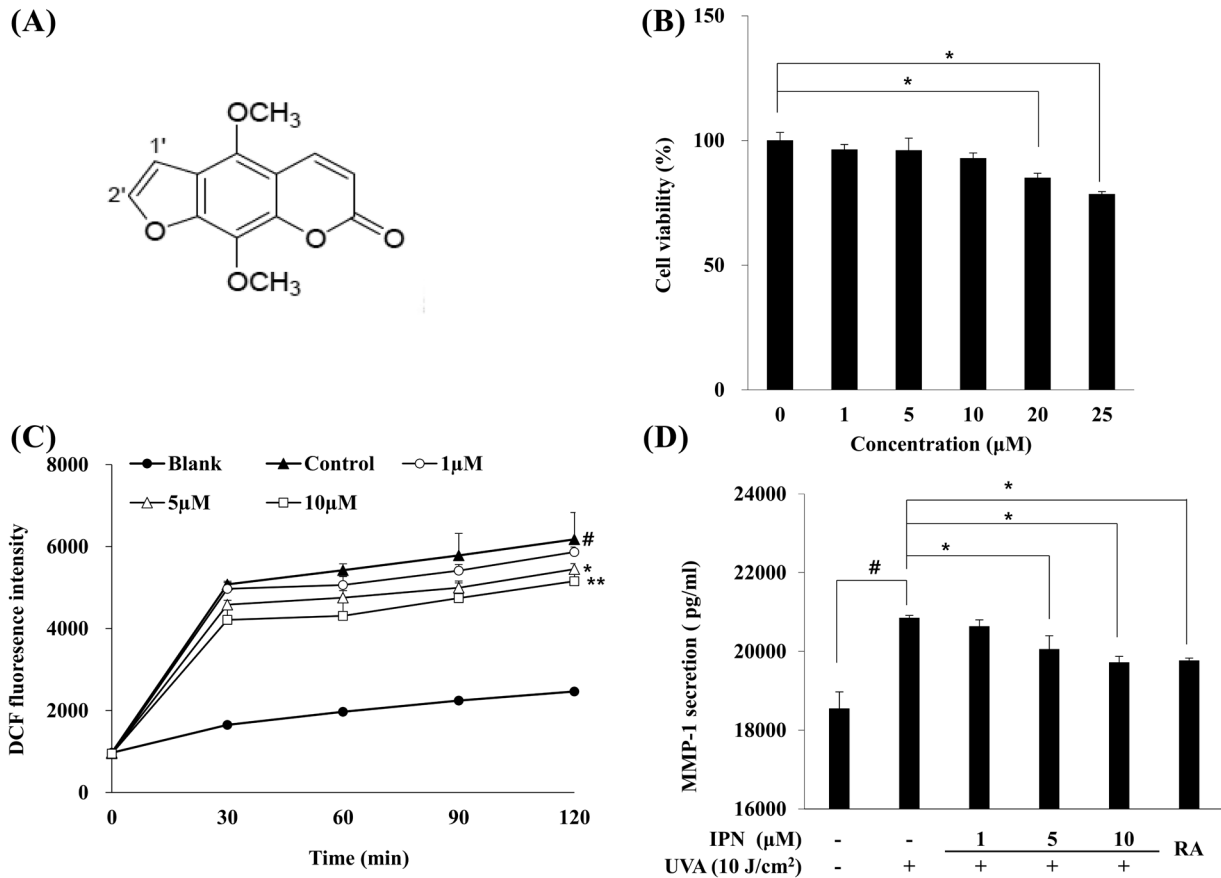


Fig. 1 (A) The chemical structure of Isopimpinellin (IPN). (B) Effect of IPN on the viability of human dermal fibroblasts (HDFs). Viability of the cells was measured after 24 h IPN treatment. Viability was given as a relative percentage of the untreated group. Values are means \pm SD ($n=3$). * $p<0.05$ vs. untreated (0 μ M) group. (C) Effect of IPN on the UVA-induced intracellular ROS levels in HDFs. HDFs were loaded with DCFH-DA and treated with or without IPN for 2 h prior to UVA irradiation. The fluorescence intensity of DCF was measured at 30 min intervals. Values are means \pm SD ($n=3$). Blank:

Non-irradiated, untreated group; Control: UVA-irradiated, untreated group. # $p<0.05$ vs. Blank, and * $p<0.05$, ** $p<0.01$ vs. Control. (D) Effect of IPN on the MMP-1 secretion of HDFs. HDFs were irradiated by UVA and treated with or without IPN for 24 h. MMP-1 levels in the cell culture medium was measured by ELISA. Values are means \pm SD ($n=3$). # $p<0.05$ vs. non-irradiated untreated group, and * $p<0.05$ vs. UVA-irradiated untreated group. RA: UVA-irradiated retinoic acid-treated (10 μ M) positive control

The HDFs were grown in black opaque 96-well plates and incubated at 37°C for 24 h prior to the assay. Following incubation, the cells were loaded with 20 μ M DCFH-DA dye (MilliporeSigma) dissolved in PBS and incubated for a further 20 min in the dark. The DCFH-DA-loaded cells were treated with or without IPN (1, 5 and 10 μ M) for 2 h. Following treatment, the cells were exposed to UVA irradiation (10 J/cm²) to induce oxidative stress. The fluorescence intensity of DCF, the end of product of DCFH-DA oxidation was measured at 30 min intervals for 2 h using a GENios® microplate reader (Tecan Group, Ltd.). The wavelengths were set at 485 nm for excitation and 528 nm for emission.

Enzyme-linked immunosorbent assay (ELISA) for the measurement of MMP-1 levels

The secreted MMP-1 levels from the UVA-irradiated HDFs were analyzed using a commercial MMP-1 ELISA kit (cat. no. DY901B, R&D systems, Inc.). The HDFs cultured as described above were incubated at 37 °C until they reached 90% confluency. The cells were washed with PBS prior to exposure to UVA at the dose described above. Following irradiation, the HDFs were treated with or without IPN at the indicated concentrations (1, 5 and 10 μ M) for 24 h. The cell culture medium was harvested from each

treatment group and the amount of MMP-1 was measured following the instructions provided with the ELISA kit.

mRNA expression levels analysed by reverse transcriptase-polymerase chain reaction (RT-PCR) for MMP expression

The HDFs were cultured, irradiated and treated with IPN as described above. The expression levels of MMP-1, -3 and -9 were analyzed using RT-PCR following 24 h of treatment. Total RNA was isolated from the HDFs using a commercial RNA extraction kit (AccuPrep® Universal, Bioneer Corporation) following the manufacturer's instructions. The RNase-free DNase I (Thermo Fisher Scientific)-treated total RNA was reverse transcribed into cDNA using CellScript All-in-One cDNA synthesis Master Mix (Cell-Safe). Target-specific cDNA amplification was carried out using traditional PCR protocols (95 °C for 45s, 60 °C for 50s, and 72 °C for 60s for 35 cycles) and gene-specific forward and reverse primers, as previously described in detail earlier (Oh et al., 2020a): MMP-1 forward, 5'-GAT-GTG-GAG-TGC-CTG-ATG-TG-3' and reverse, 5'-TGC-TTG-ACC-CTC-AGA-GAC-CT-3'; MMP-3 forward, 5'-GGA-GCC-TCT-CAG-TCA-TGG-AG-3' and reverse, 5'-TTG-AGC-TGG-ACT-CAT-TGT-CG-3'; MMP-9 forward, 5'-CAC-TGT-CCA-CCC-CTC-AGA-GC-3' and reverse, 5'-CAC-TTG-TCG-GCG-ATA-AGG; and β -actin forward, 5'-GAG-TCA-ACG-GAT-TTG-GTC-GT-3' and reverse, 5'-GAC-AAG-CTT-CCC-GTT-CTC-AG-3'. β -actin was used as a loading control.

Measurement of protein levels in UVA-irradiated HDFs

The HDFs were cultured, irradiated and treated with IPN as described above. To analyze the protein levels of MMPs, MAPK proteins and AP-1 dimers, total protein was isolated from the cells following the addition of 1 ml RIPA buffer (MilliporeSigma) to each well after removal of the media and subsequent vigorous pipetting to lyse the cells. The cell lysates were then centrifuged at 16,000 \times g for 10 min at 4 °C and the supernatants were used for western blotting. Using a BCA protein assay kit (Thermo Fisher Scientific) the protein concentration of each sample was quantified in order to load same amount of protein (20 μ g) from each group to a 10% SDS-PAGE gel. Following SDS-PAGE, the proteins were transferred from gels onto nitrocellulose membranes. The blotted membranes were then blocked in 5% skim milk for 4 h at room temperature and hybridized overnight at 4 °C with primary antibodies against MMP-1 (cat. no. sc-6837), MMP-3 (cat. no. sc-21732), MMP-9 (cat. no. sc-393859), TIMP-1 (cat. no. sc-21734), TIMP-2 (cat. no. sc-21735) (all from Santa Cruz Biotechnology, Inc.), p38 (cat. no. #8690),

p-p38 (cat. no. #4511), ERK (cat. no. #4695), p-ERK (cat. no. #4370) (all from Cell Signaling Technology, Inc.), JNK (cat. no. LF-PA0047, Thermo Fisher Scientific, Inc.), p-JNK (cat. no. #9255, Cell Signaling Technology, Inc.), c-Fos (cat. no. sc-7202, Santa Cruz Biotechnology, Inc.), p-c-Fos (cat. no. #5348s, Cell Signaling Technology, Inc.), c-Jun (cat. no. sc-74543), p-c-Jun (cat. no. sc-822), SOD-1 (cat. no. sc-11407), HO-1 (cat. no. sc-1797), Nrf-2 (cat. no. sc-30015) and β -actin (cat. no. sc-47778) (all from Santa Cruz Biotechnology, Inc.). Hybridized membranes were incubated with horseradish peroxidase conjugated anti-mouse (cat. no. #7076, Cell Signaling Technology, Inc.) and anti-rabbit (cat. no. sc-2357, Santa Cruz Biotechnology, Inc.) antibodies for 1 h at room temperature. Protein bands on membranes were visualized using a commercial chemiluminescence kit (Amersham ECL detection kit, Cytiva) and images were obtained using the Davinch-Chemi imager (CAS-400 M, Davinch-K Co., Ltd.).

Immunofluorescence staining of AP-1 levels

The intracellular levels of AP-1 dimers, c-Fos and c-Jun were also examined using immunofluorescence staining. The HDFs were cultured on glass coverslips, placed into six-well plate wells, and irradiated and treated with IPN as described above. Following 24 h of treatment, the HDFs were fixed on glass coverslips and loaded with anti-c-Fos and anti-c-Jun antibodies described above for 2 h at room temperature and subsequently attached with secondary antibodies, Alexa Fluor 488 Green (A-11008; Invitrogen), and ProLong Gold Antifade Reagent with 4',6-diamidino-2-phenylindole (DAPI) (#8961; Cell Signaling Technology, Inc.) for the detection of cell nuclei, for 1 h at room temperature. Visualization of the stained cells was carried out using a commercial Immunofluorescence Application Solutions kit (cat. no. #12727, Cell Signaling Technology, Inc.) following the manufacturer's protocol.

Statistical analysis

All numerical data are presented as the mean of three different experiments \pm SE. Significant differences between groups were determined using one-way ANOVA with Duncan's multiple range test as post hoc (SAS v9.1, SAS Institute, Inc.). A value of $p < 0.05$ was considered to indicate a statistically significant difference.

Results and discussion

In the dermis layer, HDFs are critical cells due to their role in the production of ECM components, such as collagen, fibronectin and glycans, which are crucial for skin structure,

elasticity, and moisture (Shin et al., 2019). UVA irradiation has been shown to directly damage HDFs, leading to aging symptoms in which the skin loses its elasticity and strength in addition to much-needed moisture (Salminen et al., 2022). According to previous research (Oh et al., 2020b), herein, UVA irradiation at a dose of 10 J/cm² was used to mimic the progression of photoaging in cultured HDFs.

In the present study, IPN was isolated from *C. heterocarpa*. It has been reported that the extracts and other coumarin derivatives from this plant have promising anti-photoaging properties against both UVA and UVB irradiation, which have been tested on HDFs, as well as human keratinocytes in vitro (Ahn et al., 2012; Oh et al., 2020a; Yu et al., 2021). Furanocoumarins, which include IPN, are a widely studied class of coumarins. It has been shown that a wide range of furanocoumarins are phototoxic substances, which hinders their use in cosmetics (Kriedl et al., 2020). On the other hand, there are cases in which furanocoumarins are used as UV-induced activators of melanogenesis to increase cellular UV absorption (Sumorek-Wiadro et al., 2020). Therefore, the present study aimed to further investigate the other ingredients of *C. heterocarpa* that may possess anti-photoaging activities.

IPN treatment reduced oxidative stress and decreased MMP-1 secretion

Prior to conducting in vitro experiments, any toxicity of IPN against the HDFs was examined using an MTT assay. The results revealed that a concentration of up to 10 μM IPN did not significantly affect cell viability (Fig. 1B). Therefore, further assays were performed using IPN in this concentration range.

To investigate the antioxidant potential of IPN, an intracellular ROS scavenging assay was carried out in the HDFs using the DCFH-DA assay. Oxidative stress induced by UVA irradiation was confirmed by a 150.81% increase in DCF fluorescence intensity compared to the non-irradiated cells at 2 h following UVA exposure (Fig. 1C). Treatment with IPN (10 μM) decreased the DCF intensity in a concentration-dependent manner by 16.5% of the untreated UVA-irradiated control, indicating a significant, yet slight antioxidant potential against UVA-induced oxidative stress.

The HDFs were exposed to UVA (10 J/cm²) and incubated with or without IPN for 24 h to detect the MMP-1 secretion levels. The results of ELISA revealed that after 24 h, the UVA-irradiated group exhibited notably elevated levels of MMP-1 in the cell culture medium compared to the non-irradiated untreated blank group (Fig. 1C). Treatment with IPN decreased the UVA-induced elevation of MMP-1 levels in a concentration-dependent manner compared to the UVA irradiated only group. In the UVA control group, the amount of MMP-1 was measured at 20,848.63 pg/ml,

whereas in the 10 μM IPN treatment group, this amount was recorded at 19,716.89 pg/ml, compared to 18,549.77 pg/ml in the non-irradiated untreated blank group.

IPN treatment activated cellular antioxidant mechanisms

Following the DCFH-DA assay, the antioxidant effects of IPN in the UVA-irradiated HDFs were further analyzed by investigating the protein levels of the antioxidant enzymes, SOD-1 and HO-1, along with the Nrf-2 transcription factor, which regulates the expression of these enzymes. Translocation of Nrf-2 protein into the nucleus triggers the expression of antioxidant enzymes (Jablonska-Trypuc et al., 2016). UVA irradiation significantly decreased the Nrf-2 levels, and consequently, the protein levels of the antioxidant enzymes, SOD-1 and HO-1 (Fig. 2). However, treatment with IPN at 10 μM attenuated the effects of UVA on the cellular

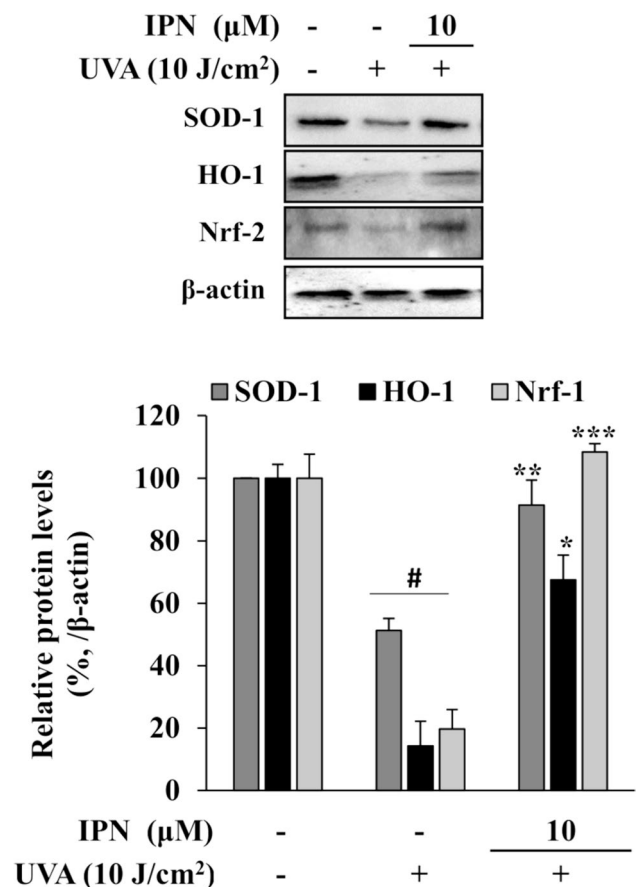


Fig. 2 Effect of IPN on protein expression levels of SOD-1, HO-1 and Nrf-2 in HDFs, analyzed by Western blot. HDFs were irradiated by UVA and treated with or without IPN for 24 h. β-actin was used as loading control. Relative protein levels were measured densitometrically and normalized against β-actin levels. #p < 0.05 vs. non-irradiated untreated group, and *p < 0.05, **p < 0.01, ***p < 0.001 vs. UVA-irradiated untreated group

antioxidant response by increasing total cellular Nrf-2 levels, which was also exhibited by an increase in the SOD-1 and HO-1 levels.

Studies have clearly demonstrated that ECM degradation upon chronic UVA exposure is a result of the activation of the MAPK/AP-1 pathway initiated by the UV-induced elevation of ROS (Fisher and Voorhees, 1998). ROS functions as a secondary messenger in intracellular cascades and therefore regulates gene expression. In this context, ECM degradation, particularly collagen degradation, is directly linked to the overexpression of MMPs. It has been reported that UV stimulates this response via ROS by suppressing the cellular antioxidant response that maintains ROS at a high level. Exposure to UVA interferes with the Nrf-2 regulated cellular antioxidant response that produces antioxidant enzymes, such as SOD-1 and HO-1 (Jablonska-Trypuc et al., 2016). In the present study, IPN was shown to facilitate the alleviation of Nrf-2 levels, as evidenced by the increased SOD-1 and HO-1 levels in the UVA-irradiated HDFs treated with IPN. The current study showed that IPN treatment increased total cellular Nrf-2 protein levels. This result indicated that the effects of IPN on the UVA-induced activation of the MAPK signaling cascade and the consequent expression of MMPs may stem from its antioxidant properties.

IPN suppressed the mRNA and protein expression of MMPs

The results of RT-PCR revealed that the mRNA levels of MMP-1, MMP-3 and MMP-9 were significantly stimulated in the HDFs following UVA irradiation compared with the non-irradiated blank group (Fig. 3A). Following treatment with 10 μ M IPN, a marked decrease was observed in the mRNA expression levels of MMP-1, MMP-3 and MMP-9.

Similar trends were observed for the protein expression levels, as determined using western blot analysis. As shown in Fig. 3B, the levels of MMP-1, MMP-3 and MMP-9 were increased in a similar manner to the mRNA levels following UVA irradiation. However, the protein levels of all tested MMPs were significantly lower in the IPN-treated groups compared with the UVA irradiated only group. In addition, the suppression of IPN-mediated MMP expression was found to be concentration-dependent.

The effect of IPN was also measured on UVA-dependent changes in the expression of TIMPs. UVA exposure reduced the protein levels of TIMP-1 and TIMP-2, which were notably elevated following treatment with 10 μ M IPN (Fig. 3C).

The MAPK/AP-1 signaling cascade is the regulatory pathway for the expression of MMPs following UV exposure. The results revealed that treatment with IPN significantly reduced the MMP-1 levels, which were elevated following UVA irradiation. The ameliorative effects of IPN on UVA-stimulated MMP-1 levels suggest a possible

anti-photoaging effect. The effect of IPN on MMP expression was then further confirmed by the results of the mRNA and protein expression levels. UVA exposure elevated the expression levels of MMP-1, MMP-3 and MMP-9, all of which degrade collagen in the ECM. IPN treatment was able to decrease the expression of all the aforementioned MMPs.

The regulation of collagen synthesis is critically dependent on the balance between the expression of collagenase-degrading MMPs and the expression of their intracellular inhibitors, TIMPs (Philips et al., 2011). It has been reported that during collagen synthesis, the levels of TIMPs are increased to reduce collagen degradation via the inhibition of MMP activity (Philips et al., 2011; Watson and Griffiths, 2005). However, during the breakdown of collagen, TIMP levels have been observed to decrease to facilitate MMP-dependent collagen degradation. Collagen synthesis and MMP-1 activity are directly related to the protein levels of TIMP-1 and TIMP-2 (Watson and Griffiths, 2005). The results of the present study revealed that UVA exposure decreased the levels of TIMP-1 and TIMP-2 in the HDFs. By contrast, treatment with IPN increased the TIMP-1 and TIMP-2 protein levels. This result suggests that IPN may regulate the diminished collagen synthesis following UV irradiation, not only by decreasing MMP expression, but also by regulating MMP activity through increased TIMP levels.

IPN treatment suppressed the activation of MAPK/AP-1 signaling

The total and phosphorylated protein levels of p38, ERK and JNK MAPKs along with their downstream targets for MMP synthesis, c-Fos, and c-Jun, were examined using western blot analysis (Fig. 4A). The results revealed that UVA irradiation notably increased the levels of p-MAPK compared to the relatively same total protein levels (Fig. 4B). Treatment with 10 μ M IPN did not significantly alter the total protein levels; however, the levels of p-p38 and p-JNK were found to be lower in the IPN-treated group compared with the UVA irradiated only group. On the other hand, IPN treatment was also found to elevate the levels of p-ERK even further.

As the downstream targets of the UVA-mediated activation of MAPK to express MMPs, the levels of AP-1 forming dimers, c-Fos and c-Jun, were also examined using western blot analysis. Similar to MAPK activation, the UVA irradiation of HDFs significantly elevated the phosphorylated protein levels of c-Fos and c-Jun, while the total protein levels remained unaltered (Fig. 4C). Following treatment with 10 μ M IPN, the levels of p-c-Fos were observed to remain the same, while those of p-c-Jun exhibited a slight decrease. This did not correspond to the IPN-induced decrease in p38 and JNK phosphorylation, respectively. However, nuclear fractions of HDFs revealed that the effect of IPN on AP-1

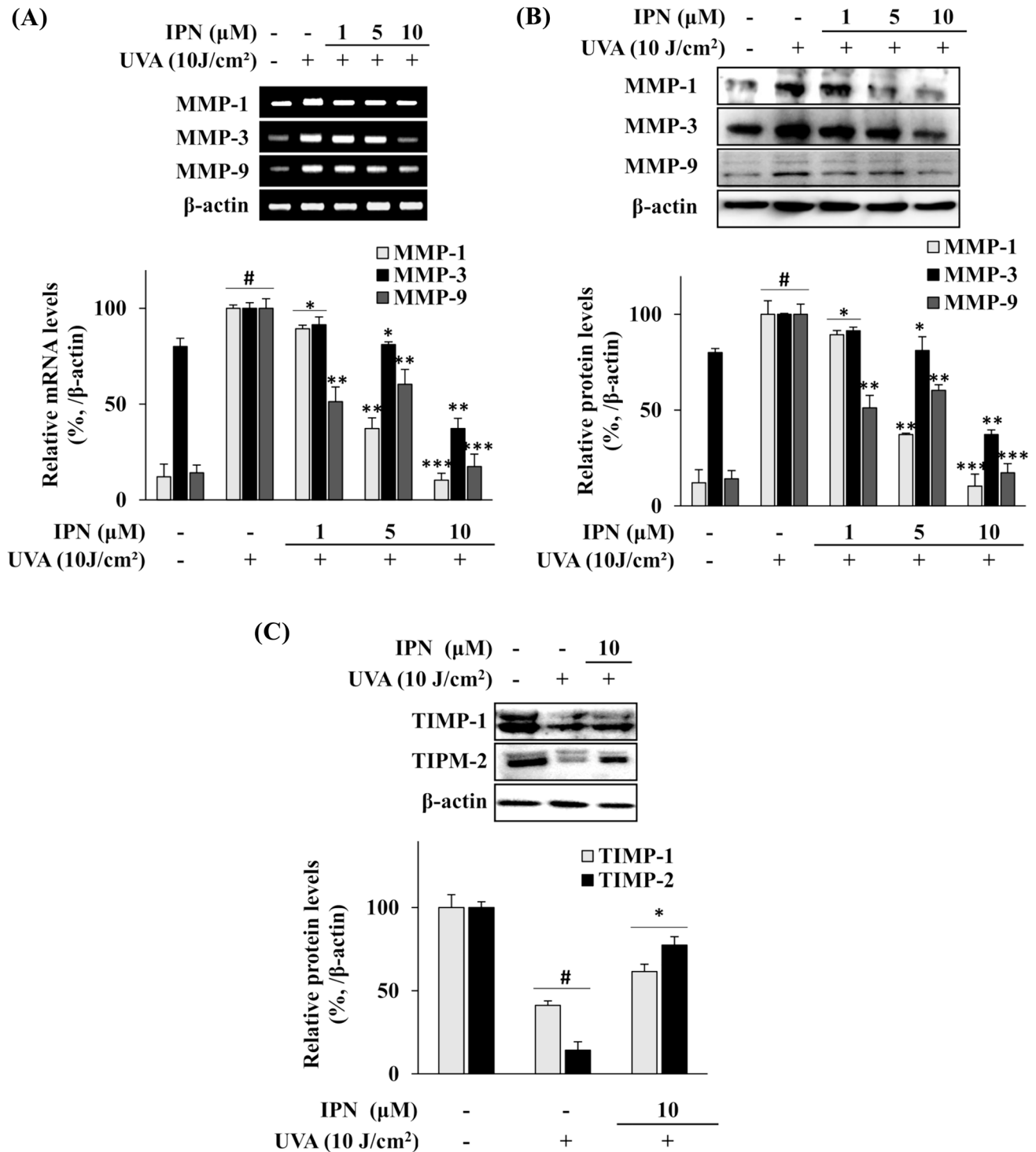


Fig. 3 Effect of IPN on the mRNA (A) and protein (B, C) expression levels of MMP-1, MMP-3, MMP-9, TIMP-1 and TIMP-2 in HDFs, analyzed by RT-PCR and Western blot analysis, respectively. HDFs were irradiated by UVA and treated with or without IPN for 24 h.

β -actin was used as loading control. Relative mRNA and protein levels were measured densitometrically and normalized against β -actin levels. # $p < 0.05$ vs. non-irradiated untreated group, and * $p < 0.05$, ** $p < 0.01$, *** $p < 0.001$ vs. UVA-irradiated untreated group

activation was present for hindering the nuclear translocation of the AP-1 building blocks, c-Fos and c-Jun. The nuclear fractions expressed significantly elevated levels of

activated (phosphorylated) c-Fos and c-Jun following UVA irradiation compared with the non-irradiated blank group (Fig. 4D). However, the IPN-treated group exhibited notably

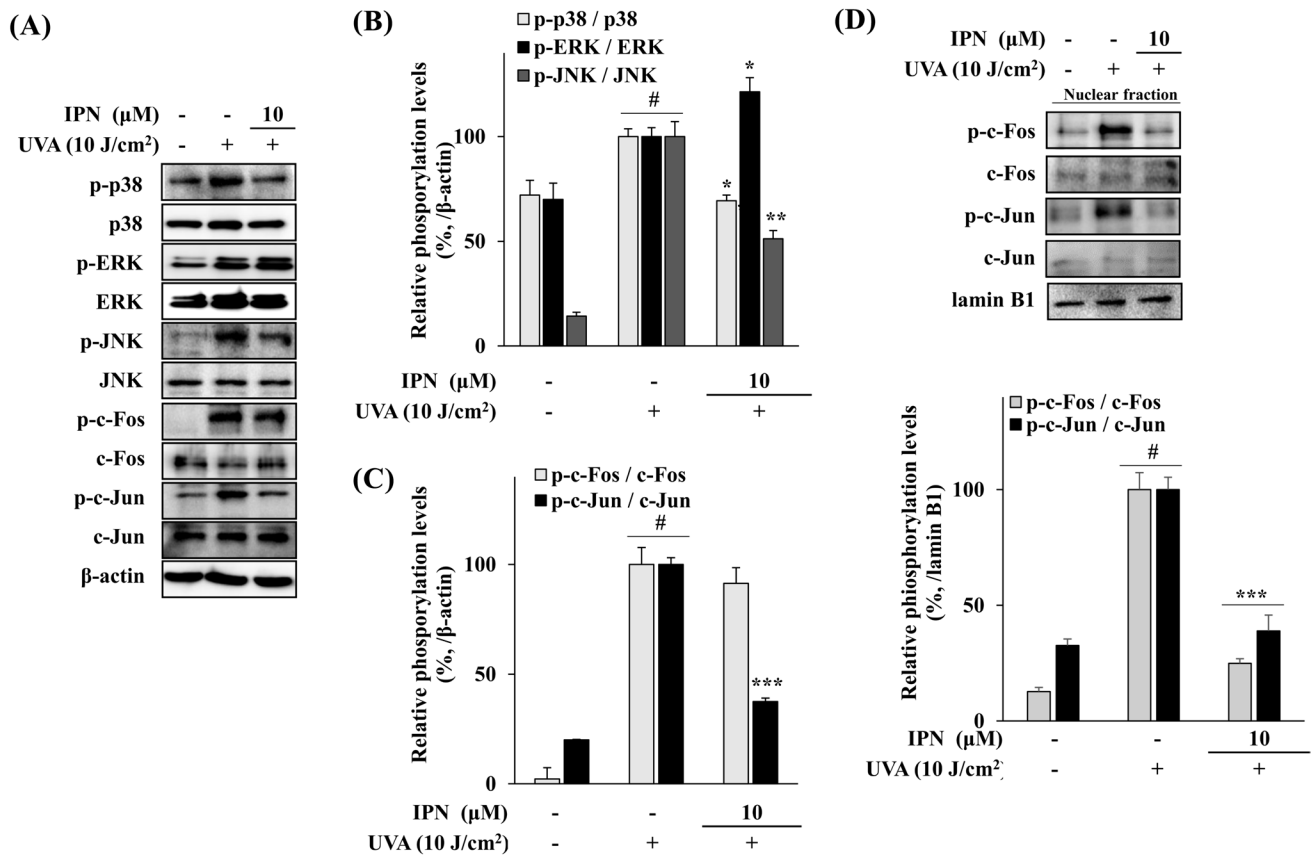


Fig. 4 Effect of IPN on the total and phosphorylated (p-) levels p38, ERK and JNK MAPKs and AP-1 dimers c-Fos and c-Jun (A) in HDFs analyzed by Western blot. HDFs were irradiated by UVA and treated with or without IPN for 24 h. β-actin was used as loading control for total cell lysates (A) and lamin B1 was used for loading

control for nuclear fractions (D). Relative protein levels were measured densitometrically and normalized against β-actin (B, C) and lamin B1 (D) levels. #p < 0.05 vs. non-irradiated untreated group, and *p < 0.05, **p < 0.01, ***p < 0.001 vs. UVA-irradiated untreated group

lower levels of activated AP-1 dimers compared to the UVA irradiated only group.

The intracellular levels of p-c-Fos and p-c-Jun in the HDFs were also investigated using fluorescence staining of the cells. As shown in Fig. 5, the UVA-mediated elevation in the c-Jun levels was significantly reversed following treatment with 10 μM IPN, whereas the c-Fos levels were in parallel with the total p-c-Fos levels observed in western blot analysis (Fig. 4B).

It has been reported that the UV radiation-induced activation of MAPK occurs via the phosphorylation of p38 and JNK MAPKs (Tanos et al., 2005). These MAPKs then phosphorylate c-Fos and c-Jun, respectively, which form the AP-1 heterodimer upon activation (Tanos et al., 2005). The subsequent translocation of activated AP-1 to the nucleus initiates the expression of MMPs. This cascade was further observed in the present study by the increased phosphorylation levels of MAPKs and AP-1 dimers following UVA exposure. The presence of IPN following exposure decreased the phosphorylation levels of p38 and JNK along

with the cellular and nuclear levels of c-Fos and c-Jun, further confirming that IPN treatment suppresses the activation of AP-1-mediated MMP expression. The results of the present study suggest that IPN reduces MMP production in UVA-irradiated HDFs by inhibiting the activation of the MAPK/AP-1 pathway.

IPN is a furocoumarin with reported bioactivities. Similarly, several other furocoumarins were reported for their anti-MMP and MAPK inhibitory activities such as angelicin (Mahendra et al., 2020), bergaptol (Widelski et al., 2017), and psoralen (Tripathi et al., 2023) all of which also inhibited either MMP expression directly or through MAPK regulation. Some studies also employed in vivo models to test the downregulatory abilities of these coumarin derivatives on MMPs or related upstream signaling pathways (Ahmed et al., 2020). In this context, Robertson et al. (2016) reported that IPN inhibited PI3K activation to exert anti-migration effects on neutrophils in a zebrafish model in relation to the roles of MMPs in the recruitment of neutrophils (Song et al., 2013). It has been

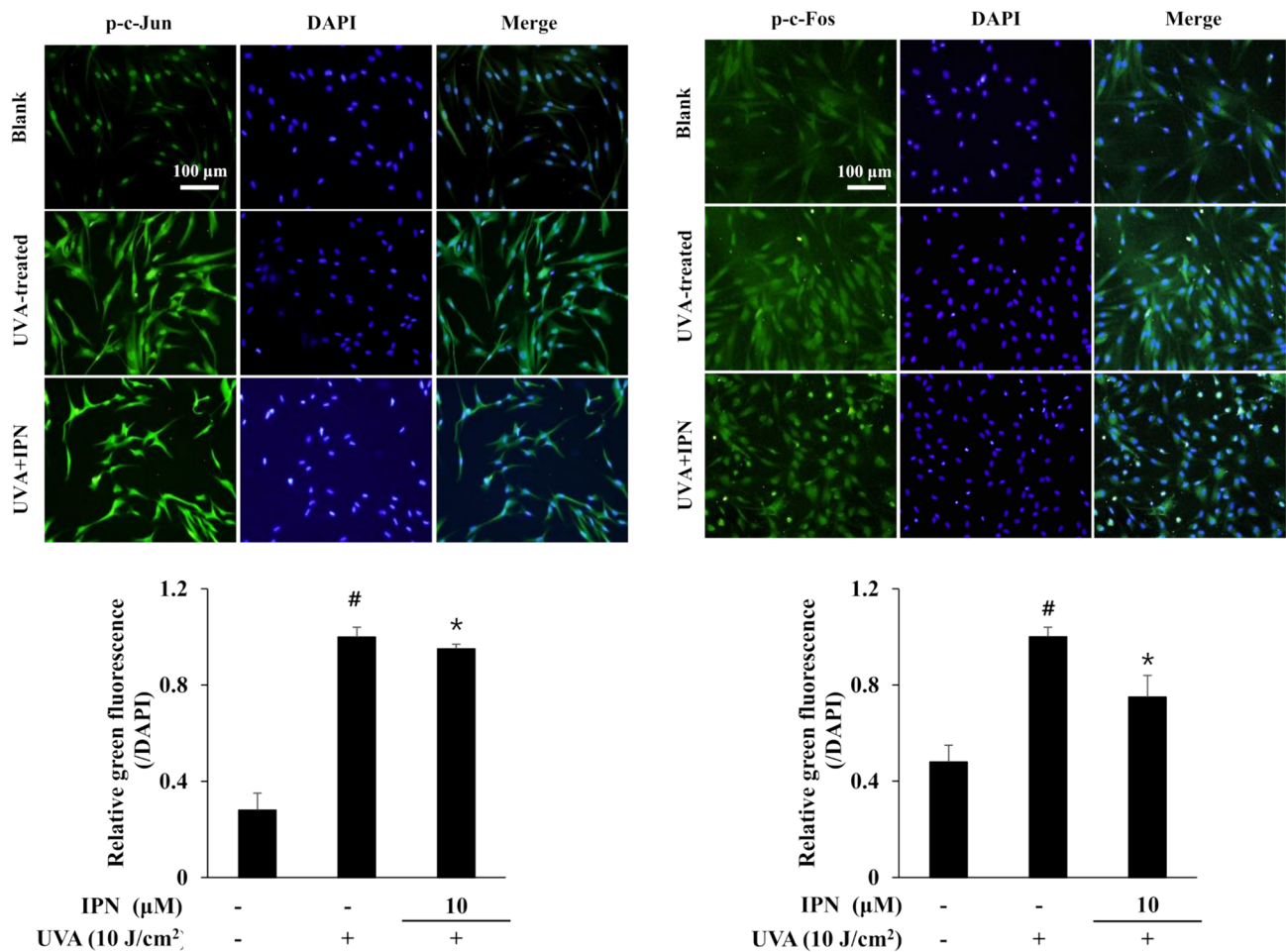


Fig. 5 Effect of IPN (10 μM) on the levels of phosphorylated (p-) c-Fos and c-Jun in HDFs. Intracellular levels of p-c-Fos and p-c-Jun were stained with immunofluorescence staining (green) and the nuclei of HDFs were stained with DAPI (blue) as viable cell control.

Relative green fluorescence was measured densitometrically and normalized against DAPI (blue) staining. #p < 0.05 vs. non-irradiated untreated group, and *p < 0.05 vs. UVA-irradiated untreated group

shown that PI3K and JNK activation are directly linked to MMP-2 expression via AP-1 (Ispanovic and Haas, 2006). The results of the current study were in accordance with the Robertson et al. (2016) data, further indicating that IPN might show in vivo efficiency to downregulate MMP expression via JNK and/or its upstream effector inhibition such as PI3K.

In conclusion, the present study demonstrated that IPN alleviated the effects induced by UVA on MMP production in HDFs. The inhibition of the MAPK/AP-1 signaling cascade via the suppression of p38 and JNK phosphorylation has been proposed as a possible mechanism of action for the suppressive effect of IPN on MMPs. The results presented herein suggest that IPN and its source, *C. heterocarpa*, may serve as cosmeceutical agents following further in vitro and in vivo experiments that confirm its anti-photoaging properties.

Acknowledgements NMR spectral data were kindly provided by Eun-Hee Kim (Korea Basic Science Institute, Daejeon, Republic of Korea).

Funding This research was supported by the BB21plus funded by Busan Metropolitan City and Busan Techno Park. This work was supported by the National Research Foundation of Korea (NRF) grant funded by the Korea government (MSIT) (No. NRF-2023R1A2C1006268 and RS-2023-00212560).

Data availability The data used to support the findings of this study are available from the corresponding author upon reasonable request.

Declarations

Competing interests The authors declare that they have no competing interests.

References

- Ahmed S, Khan H, Aschner M, Mirzae H, Kùpeli Akkol E, and Capasso R. Anticancer potential of furanocoumarins: Mechanistic and therapeutic aspects. *International Journal of Molecular Sciences*. 21: 5622 (2020)
- Ahn B-N, Kim J-A, Kong C-S, Seo Y, Kim S-K. Protective effect of (2'S)-columbianetin from *Corydalis heterocarpa* on UVB-induced keratinocyte damage. *Journal of Photochemistry and Photobiology B: Biology*. 109: 20-27 (2012)
- Ansary TM, Hossain MR, Kamiya K, Komine M, Ohtsuki M. Inflammatory molecules associated with ultraviolet radiation-mediated skin aging. *International Journal of Molecular Sciences*. 22: 3974 (2021)
- Battie C, Jitsukawa S, Bernerd F, Del Bino S, Marionnet C, Verschoore M. New insights in photoaging, UVA induced damage skin types. *Experimental Dermatology*. 23: 7-12 (2014)
- Bhagavatheswaran S, Ramachandran V, Shanmugam S, Balakrishnan A. Isopimpinellin extends antiangiogenic effect through overexpression of miR-15b-5p downregulating angiogenic stimulators. *Molecular Biology Reports*. 49: 279-291 (2022)
- Fisher GJ, Voorhees JJ. Molecular mechanisms of photoaging and its prevention by retinoic acid: ultraviolet irradiation induces MAP kinase signal transduction cascades that induce Ap-1-regulated matrix metalloproteinases that degrade human skin in vivo. *Journal of Investigative Dermatology Symposium Proceedings*. 3: 61-68 (1998)
- Herrling T, Jung K, Fuchs J. Measurements of UV-generated free radicals/reactive oxygen species (ROS) in skin. *Spectrochimica Acta Part A: Molecular and Biomolecular Spectroscopy*. 63: 840-845 (2006)
- Herrmann G, Wlaschek M, Lange TS, Prenzel K, Goerz G, Scharfetter-Kochanek K. UVA irradiation stimulates the synthesis of various matrix-metalloproteinases (MMPs) in cultured human fibroblasts. *Experimental Dermatology*. 2: 92-97 (1993)
- Ispanovic E, and Haas TL. JNK and PI3K differentially regulate MMP-2 and MT1-MMP mRNA and protein in response to actin cytoskeleton reorganization in endothelial cells. *American Journal of Physiology-Cell Physiology*. 291: C579-C588 (2006)
- Jabłońska-Trypuć A, Matejczyk M, Rosochacki S. Matrix metalloproteinases (MMPs), the main extracellular matrix (ECM) enzymes in collagen degradation, as a target for anticancer drugs. *Journal of Enzyme Inhibition and Medicinal Chemistry*. 31: 177-183 (2016)
- Kajanne R, Miettinen P, Mehlem A, Leivonen S-K, Birrer M, Foschi M, Kähäri V-M, Leppä S. EGF-R regulates MMP function in fibroblasts through MAPK and AP-1 pathways. *Journal of Cellular Physiology*. 212: 489-497 (2007)
- Kim Y, Kong C-S, Park H, Lee E, Jang M-S, Nam K-H, Seo Y. Anti-inflammatory activity of heterocarpin from the salt marsh plant *corydalis heterocarpa* in LPS-induced RAW 264.7 Macrophage Cells. *Molecules*. 20: 14474-14486 (2015)
- Kleiner HE, Reed MJ, DiGiovanni J. Naturally occurring coumarins inhibit human cytochromes P450 and block benzo[a]pyrene and 7,12-dimethylbenz[a]anthracene DNA adduct formation in MCF-7 cells. *Chemical Research in Toxicology*. 16: 415-422 (2003)
- Kleiner HE, Vulimiri S V., Starost MF, Reed MJ, DiGiovanni J. Oral administration of the citrus coumarin, isopimpinellin, blocks DNA adduct formation and skin tumor initiation by 7,12-dimethylbenz[a]anthracene in SENCAR mice. *Carcinogenesis*. 23: 1667-1675 (2002)
- Kong L, Barber T, Aldinger J, Bowman L, Leonard S, Zhao J, Ding M. ROS generation is involved in titanium dioxide nanoparticle-induced AP-1 activation through p38 MAPK and ERK pathways in JB6 cells. *Environmental Toxicology*. 37: 237-244 (2022)
- Kreidl M, Rainer M, Jakschitz T, Bonn GK. Determination of phototoxic furanocoumarins in natural cosmetics using SPE with LC-MS. *Analytica Chimica Acta*. 1101: 211-221 (2020)
- Mahendra CK, Tan LTH, Lee WL, Yap WH, Pusparajah P, Low LE, Tang SY, Chan KG, Lee LH, and Goh BH. Angelicin—A furanocoumarin compound with vast biological potential. *Frontiers in Pharmacology*. 11: 366 (2020)
- Meinhardt M, Krebs R, Anders A, Heinrich U, Tronnier H. Wavelength-dependent penetration depths of ultraviolet radiation in human skin. *Journal of Biomedical Optics*. 13: 044030 (2008)
- Narayanan DL, Saladi RN, Fox JL. Review: Ultraviolet radiation and skin cancer. *International Journal of Dermatology*. 49: 978-986 (2010)
- Nelson KK, Melendez JA. Mitochondrial redox control of matrix metalloproteinases. *Free Radical Biology and Medicine*. 37: 768-784 (2004)
- Oba A, Edwards C. Relationships between changes in mechanical properties of the skin, wrinkling, and destruction of dermal collagen fiber bundles caused by photoaging. *Skin Research and Technology*. 12: 283-288 (2006)
- Oh JH, Karadeniz F, Lee JI, Kim HR, Seo Y, Kong C-S. Antiphotoprotective effect of (2'S)-columbianetin from *Corydalis heterocarpa* in UVA-irradiated human dermal fibroblasts. *Applied Sciences*. 10: 2568 (2020)
- Oh JH, Karadeniz F, Lee JI, Park SY, Seo Y, Kong C-S. Anticatabolic and anti-inflammatory effects of myricetin 3-O-β-D-galactopyranoside in UVA-irradiated dermal cells via repression of MAPK/AP-1 and activation of TGFβ/Smad. *Molecules*. 25: 1331 (2020)
- Philips N, Auler S, Hugo R, Gonzalez S. Beneficial regulation of matrix metalloproteinases for skin health. *Enzyme Research*. 2011: 1-4 (2011)
- Pittayapruek P, Meehansan J, Prapapan O, Komine M, Ohtsuki M. Role of matrix metalloproteinases in photoaging and photocarcinogenesis. *International Journal of Molecular Sciences*. 17: 868 (2016).
- Poon F, Kang S, Chien AL. Mechanisms and treatments of photoaging. *Photodermatology, Photoimmunology & Photomedicine*. 31: 65-74 (2015)
- Prasanth MI, Gayathri S, Bhaskar JP, Krishnan V, Balamurugan K. Understanding the role of p38 and JNK mediated MAPK pathway in response to UV-A induced photoaging in *Caenorhabditis elegans*. *Journal of Photochemistry and Photobiology B: Biology*. 205: 111844 (2020)
- Quan T, Qin Z, Xia W, Shao Y, Voorhees JJ, Fisher GJ. Matrix-degrading metalloproteinases in photoaging. *Journal of Investigative Dermatology Symposium Proceedings*. 14: 20-24 (2009)
- Robertson AL, Ogryzko N V., Henry KM, Loynes CA, Foulkes MJ, Meloni MM, Wang X, Ford C, Jackson M, Ingham PW, Wilson HL, Farrow SN, Solari R, Flower RJ, Jones S, Whyte MKB, and Renshaw SA. Identification of benzopyrone as a common structural feature in compounds with anti-inflammatory activity in a zebrafish phenotypic screen. *Disease Models & Mechanisms*. 9: 621-632 (2016)
- Salminen A, Kaarniranta K, Kauppinen A. Photoaging: UV radiation-induced inflammation and immunosuppression accelerate the aging process in the skin. *Inflammation Research*. 71: 817-831 (2022)
- Shin J-W, Kwon S-H, Choi J-Y, Na J-I, Huh C-H, Choi H-R, Park K-C. Molecular mechanisms of dermal aging and antiaging approaches. *International Journal of Molecular Sciences*. 20: 2126 (2019)
- Singhuber J, Baburin I, Ecker GF, Kopp B, Hering S. Insights into structure-activity relationship of GABAA receptor modulating coumarins and furanocoumarins. *European Journal of Pharmacology*. 668: 57 (2011)

- Song J, Wu C, Zhang X, and Sorokin LM. In vivo processing of CXCL5 (LIX) by matrix metalloproteinase (MMP)-2 and MMP-9 promotes early neutrophil recruitment in IL-1 β -induced peritonitis. *The Journal of Immunology*. 190: 401-410 (2013)
- Sumorek-Wiadro J, Zając A, Maciejczyk A, Jakubowicz-Gil J. Furanocoumarins in anticancer therapy - For and against. *Fitoterapia*. 142: 104492 (2020)
- Takomthong P, Waiwut P, Yenjai C, Sripanidkulchai B, Reubroycharoen P, Lai R, Kamau P, Boonyarat C. Structure-activity analysis and molecular docking studies of coumarins from *Toddalia asiatica* as multifunctional agents for Alzheimer's disease. *Biomedicine*. 8: 107 (2020)
- Tanos T, Marinissen MJ, Leskow FC, Hochbaum D, Martinetto H, Gutkind JS, Coso OA. Phosphorylation of c-Fos by members of the p38 MAPK family. *Journal of Biological Chemistry*. 280: 18842-18852 (2005)
- Tripathi N, Bhardwaj N, Kumar S, and Jain SK. Phytochemical and pharmacological aspects of psoralen – A bioactive furanocoumarin from *Psoralea corylifolia* Linn. 20: e202300867 (2023)
- Wang M, Lei M, Chang L, Xing Y, Guo Y, Pourzand C, Bartsch JW, Chen J, Luo J, Widya Karisma V, Nisar MF, Lei X, Zhong JL. Bach2 regulates autophagy to modulate UVA-induced photoaging in skin fibroblasts. *Free Radical Biology and Medicine*. 169: 304-316 (2021)
- Watson REB, Griffiths CEM. Pathogenic aspects of cutaneous photoaging. *Journal of Cosmetic Dermatology*. 4: 230-236 (2005)
- Widelski J, Kukula-Koch W, Baj T, Kedzierski B, Fokialakis N, Magiatis P, Pozarowski P, Rolinski J, Graikou K, Chinou I, and Skalicka-Wozniak K. Rare coumarins induce apoptosis, G1 cell block and reduce RNA content in HL60 cells. *Open Chemistry*. 15: 1-6 (2017)
- Yu GH, Karadeniz F, Kong C-S. MMP-2 and MMP-9 inhibitory effects of different solvent fractions from *Corydalis heterocarpa*. *Journal of Life Science*. 31: 980-986 (2021)

Publisher's Note Springer Nature remains neutral with regard to jurisdictional claims in published maps and institutional affiliations.

Springer Nature or its licensor (e.g. a society or other partner) holds exclusive rights to this article under a publishing agreement with the author(s) or other rightsholder(s); author self-archiving of the accepted manuscript version of this article is solely governed by the terms of such publishing agreement and applicable law.